

EVALUATION AND TESTING OF THE ZEISS SCAI ROLL FILM SCANNER

Emmanuel P. Baltasvias^a, Christoph Käser^b

^aInstitute of Geodesy and Photogrammetry, ETH-Hoenggerberg, CH-8093 Zurich, Switzerland, manos@geod.ethz.ch

^bSwiss Federal Office of Topography, Seftigenstr. 264, CH-3084 Wabern, Switzerland, Christoph.Kaaser@lt.admin.ch

Commission I, Working Group 1

KEY WORDS: Roll Film Scanner, Film Digitisation, Scanner Quality Analysis, Scanner Test Patterns, Scanner Calibration.

ABSTRACT

In the summer of 1996 the Swiss Federal Office of Topography (L+T) performed in cooperation with ETH benchmark tests at different companies in order to evaluate three photogrammetric film scanners. After the tests a Zeiss SCAI scanner was acquired, installed, and tested in spring 1997 as to whether it fulfils the contract specifications. In this paper the results of these two tests performed with the SCAI, and in particular geometric and radiometric investigations, are presented. Good quality test patterns and accurate processing methods for their performance evaluation have been employed. The geometric tests include geometric errors, misregistration between colour channels, geometric repeatability, and determination of the geometric resolution. The radiometric tests include investigations on noise, linearity, dynamic range, spectral variation of noise, and artifacts. After a brief description of the scanner, details on the above investigations, analysis methods and results are presented. Regarding the geometric accuracy the RMS was 2.0-2.3 μm and the mean maximum absolute error 6.0-8.1 μm . The errors are bounded, i.e. the maximum absolute error is 2.7-3.6 RMS. Systematic co-registration errors in scan direction between the colour channels of up to ca. 2.5 μm have been observed. The short term repeatability was very high. The radiometric noise level is 1-1.6 and 0.9-1.3 grey values for 7 and 14 μm scan pixel size respectively. The dynamic range is 1.6-1.9D and 1.75-2.05D for 7 and 14 μm respectively with a good linear response up to this value. Quite a lot of artifacts and electronic noise up to 5 grey values were observed. There were no significant differences between R, G, B channels with respect to geometry but their radiometric behaviour was quite different. The software is generally positive but improvements regarding automatic density determination, geometric and radiometric calibration, and user freedom in scan parameter choice are needed.

1. INTRODUCTION

PHODIS SC is part of the PHODIS family of digital photogrammetric products by Zeiss. It consists of three main modules: scanner, roll film attachment, and user interface. A description of PHODIS SC is given in Mehlo, 1995 and Roth, 1996. Here, only its main characteristics are given. The scanner is flatbed with stationary stage and moving sensor, optics and illumination and can scan colour in one pass. The sensor is a Thomson THX7821 CCC trilinear colour CCD with 8640 elements, out of which only the 5632 central are used, while the sensor element size is 7 μm . The pairwise distance between the single CCDs is known with an accuracy of < 1 μm and is 294 μm (i.e. corresponds to 42 pixels with 7 μm scan pixel size) and the sequence of the scan is B, G, R. Grey values are generated in 12-bit and are stored with 12- or usually 8-bit through a linear or user-defined LUT. According to manufacturer statements for each CCD line there is a separate read-out register and A/D converter. Films are scanned combwise in swaths (for an aerial image 6 swaths are needed). The swaths are not overlapping, and no radiometric correction to avoid differences between neighbouring swaths is performed. The maximum scan format is 250 (y) x 275 (x) mm. The scanning mechanism has a primary (x) and a secondary (y) carriage. The optics consists of a lightweight achromatic mirror lens with zero distortion. The light source is a stabilised 250 W halogen lamp positioned away from the scanner stage and the CCD. The light is conducted over the scanner stage with fiber glass optics and is diffused before illuminating the film. The scan pixel size is 7, 14, 28, ...224 μm . Scanning with 21 μm is also possible (but not with 35 or 42 μm which could be useful for certain applications). The generation of pixel sizes other than 7 μm is achieved, in the scan direction by

increasing appropriately the scan speed and in the CCD line by pixel averaging. Its specified geometric accuracy (standard deviation) is better than 2 μm , and the radiometric one 1.5 grey values, while the density range is 0-3D. The scan speed range is from 0.35 mm/s to 38 mm/s, and the exposure time 0.2-25.5 ms (default 2 ms). The scanner throughput is ca. 1. MB/s for 14 μm scans, while with 7 μm and colour scans ca. 4 MB/s can be generated. The internal image buffer is only 4 MB, thus the data must be transferred to host and saved on disk fast enough, so that no data losses occur. Monochrome scans are possible but it is unknown whether for this purpose the signal is taken from one CCD or a specific combination of all three. Colour images can be scanned as B/W with various predefined or user-definable weighted combinations of the R, G, B values. The scanner has an autowinder option for digitising roll film of 241 mm width and up to 150 m length with manual or automatic transport. SCAI has an internal computer (Compaq, Intel Pentium, 100 MHz, 8 MB RAM), while the host computer is a UNIX Silicon Graphics, currently with a fast SCSI-II interface. The same scanner is also sold by Intergraph, whereby the software is different and runs under Windows NT.

The scanner performs for each element of each CCD a radiometric calibration. The so called normalisation (or white adjustment) uses a special slit and ensures that all sensor elements produce same grey values for a homogeneous grey surface. If the calibration slit is not absolutely clean, then the corrections are wrong. This calibration can optionally be performed before each scan, however at L+T it is not performed frequently. The so called black adjustment uses the values of 1000 light-protected sensor elements each to the left and right of the central 5632 elements. From the white and black adjustment,

gain and offset correction factors are computed for each CCD sensor element such that their response becomes equal. The gains and offsets are used to precompute LUTs which are applied during the A/D conversion (it is not clear whether the corrections are applied to the analogue or digital image signal). A geometric calibration can also be performed. Its aim is (a) to determine the rotation between CCD lines and scanner stage coordinate system as well as nonorthogonality between the x and y stage coordinate system by scanning a horizontal line in two swaths, and (b) overlaps or gaps in the x-direction between two neighbouring scan swaths by scanning a diagonal line. Thereby, it is assumed that the scanner has an accurate positioning in x and y, and that the two scale factors (pixel size) are known. The measurements for the calibration are manual or semiautomatic. A grid plate up to 4.5 mm thickness can be used for evaluation of the geometric accuracy. The documentation does not mention, except when moving the scanner at another place, how often the geometric calibrations should be performed.

2. TEST PROCEDURES AND TEST PATTERNS

The geometric and radiometric investigations were performed with two SCAI scanners, one at Zeiss Oberkochen during the benchmark test (called SCAI1 thereafter) and one at L+T after delivery and installation (called SCAI2). In both cases all necessary scanner calibration procedures were performed in advance. The host computer was a Silicon Graphics, in the second test an Indy 2. Both scanners were equipped with a roll film transport system but no roll film was mounted on it.

The geometric performance was tested by scanning with 14 μm a custom-made glass grid plate, produced by a Swiss company specialising in high precision optical components (IMT) with a 1 cm grid spacing and 187.5 μm line width (25 x 25 lines, their intersections will be called crosses thereafter). The coordinates of the crosses were known with an accuracy of 2 - 3 μm . To determine the scanner resolution a standard USAF resolution pattern on glass produced by Heidenhain was scanned with 7 μm . The radiometric performance was mainly checked by scanning a calibrated Kodak CAT grey level wedge on film (21 densities with density step of approximately 0.15D; density range 0.05D-3.09D). The densities were determined by repeated measurements using a Gretag D200 microdensitometer. In addition, a B/W and a colour (only for SCAI1) aerial image were scanned with 14 μm in order to check the visual quality and possible radiometric artifacts. The grid plate was scanned in colour, once with SCAI1 and three times with SCAI2, to check the misregistration between the colour channels as well as the short term geometric repeatability. The grey level wedge was scanned in colour, with 7 and 14 μm pixel size to check differences between colour channels and the effect of pixel size on the radiometric performance. With SCAI1 the 7 μm scan was additionally sub-sampled to 14 μm by averaging 2 x 2 pixels (called version 2) and compared to the original 14 μm scan (version 1). With SCAI2 the 14 μm scan was done twice by using exposure times of 17 and 6 (units are relative).

The pixel coordinates of the grid crosses were measured by Least Squares Template Matching (LSTM) using a 27x27 pixel template. This algorithm is described in Gruen, 1985 and details can be found in Baltsavias, 1991. The accuracy of LSTM, as indicated by the standard deviations of the shifts, was for these targets 0.01 - 0.03 pixels. Matching results with bad quality criteria (low crosscorrelation coefficient etc.) were excluded

from any further analysis. In addition, the matching results of all crosses with large errors were interactively controlled.

The geometric tests performed include:

1. Geometric tests

For this purpose an affine transformation between the pixel and the reference coordinates of all crosses was computed with three versions of control points (all crosses, 8 and 4, the latter two versions simulating the fiducial marks used in the interior orientation of aerial images).
2. Misregistration errors between the channels

Such errors were checked by comparing pairwise the pixel coordinates of each channel (R-G, R-B, G-B).
3. Repeatability

It was checked by comparing the results between different scans (short term repeatability with SCAI2) and the results of the two scanners.
4. Geometric resolution

It was determined by visual inspection of the scanned resolution pattern, i.e. the smallest line group that was discernible was detected, whereby it was required that the contrast between lines is homogeneous along the whole line length.

The radiometric tests include:

1. Estimation of the noise level, linearity, dynamic range and spectral variation of noise

This was done by determining the mean and standard deviation for each density of the grey level wedge. The number of samples per density was 568,000 and 142,000 for the 7 and 14 μm scans respectively. In previous tests it has been noticed that the grey level wedges of our film, especially for the high densities, are not homogeneous, i.e. they are lighter towards the borders. To avoid influence of such inhomogeneities on the computed grey level statistics only the central region of each wedge was used (the same region for all wedges and test scans, independently of the scan pixel size). In addition, in the first test when scanning with 7 μm pixel size a corn pattern was visible, particularly for low densities. To reduce the effect of such dark corn and also of dust etc., grey values that are outside a range are excluded from the computation of the statistics. The range is computed for each grey wedge as (mean \pm 3 x standard deviation), whereby the minimum and maximum allowable range is 4 and 20 grey values respectively. The minimum range is used to avoid excluding too many pixels in high density wedges with small standard deviation due to saturation. The linearity was checked by plotting the logarithm of the mean grey value of each wedge against the respective calibrated density. These points should ideally lie along a line and be equidistant. The dynamic range is determined as following. Firstly, the minimum unsaturated density is selected. Then, the maximum detectable density "i" is determined using the following conditions:

(a) $M_{i+1} + SD_{i+1} + SD_i < M_i < M_{i-1} - SD_{i-1} - SD_i$, with M and SD the mean and standard deviation of the wedges and "i" increasing with increasing density (i.e. the distance of the mean grey value of a detectable density from the mean values of its two neighbouring densities must be at least equal to the sum of the SD of the detectable density and the SD of each of its neighbours), (b) $SD_i > 0.1$ (to avoid cases when other conditions, especially condition a), are fulfilled but the

signal is in reality saturated and therefore has a very small SD), and (c) $nint(M_i) \neq nint(M_j)$, with "j" any other density except "i" (i.e. since grey values are integer the mean grey value of a detectable density must differ from the mean grey value of all other densities).

2. Artifacts

Some of the above mentioned scanned patterns as well as the aerial films were very strongly contrast-enhanced by Wallis filtering (Baltasvias, 1991). This permits the visual detection of various possible artifacts like radiometric differences between neighbouring swaths, electronic noise, etc. However, the quantification of radiometric errors is always performed using the original images.

3. EVALUATION OF GEOMETRIC PERFORMANCE

3.1. Geometric Accuracy and Repeatability

In all geometric tests x is the direction of the CCD line, y the scan direction. The results of this evaluation are shown in Table 1 and some examples are illustrated in Figure 1. The transformation with 8 control points (CP) was left out from the table to make it more readable. Generally, they were slightly better than the results with 4 CP (for SCAI1 2% higher RMS in x and 27% lower RMS in y , for SCAI2 9% lower RMS in x and same RMS in y).

First, the results using all crosses as control points are examined. The differences in accuracy between R, G, B is negligible. This means that the optical system has good achromatic properties. It is also due to the fact that the 3 channels are acquired quasi simultaneously (there is only an offset of 42 pixels between CCD-lines in scan direction). With both scanners RMS values are similar in x - and y -direction and vary between 2 and 2.3 μm . However, the maximum absolute errors are higher in y than in x

for SCAI1 (which is what was expected since the geometry in scan direction should be less stable) but higher in x for SCAI2. Otherwise, both scanners show very similar RMS values and also range of maximum absolute errors. Latter are bounded and the average for all channels in x/y is 2.7/3.6 RMS (SCAI1) and 3.5/3.2 RMS (SCAI2). The short term repeatability, as indicated by the difference between minimum and maximum values of the 3 scans with SCAI2 (see Table 1), is very good. The error patterns as shown in Figure 1 are for the red channel of SCAI1 and SCAI2 respectively. There were very little differences in the error patterns between the 3 channels and also between the 3 scans (SCAI2). As it can be seen, the error patterns differ from scanner to scanner, from one scan swath to another, and even within one scan swath. Thus, it is difficult to interpret them and relate them to specific error sources, e.g. vibrations, mechanical positioning, calibration errors etc. However, in both scans local systematic error patterns can be observed, as well as slightly increasing errors in the lower half of the scans, i.e. away from the home position of the scanner.

The results using only 4 control points were, as expected, worse but in accordance with the above statements. The RMS in x/y are (2.2 - 2.3)/(2.9 - 3.3) for SCAI1 and (2.4-3.2)/(2.2-2.4) for SCAI2. The mean maximum absolute errors in x/y were (5.9-6.0)/(6.9-8.0) for SCAI1 and (7.5-7.8)/(6.4-6.5) for SCAI2. A problem is the high mean y value for SCAI1 and mean x value for SCAI2 showing a systematic bias, for SCAI1 even larger than half the RMS.

The blue channel of the grid plate, the S/W aerial film and the blue channel of the colour aerial film (latter only for SCAI1) were subsampled and strongly contrast-enhanced by Wallis filtering. Then, the borders between scan swaths were visually controlled to detect geometric shifts and radiometric differences between the swaths. However, no such problems could be observed.

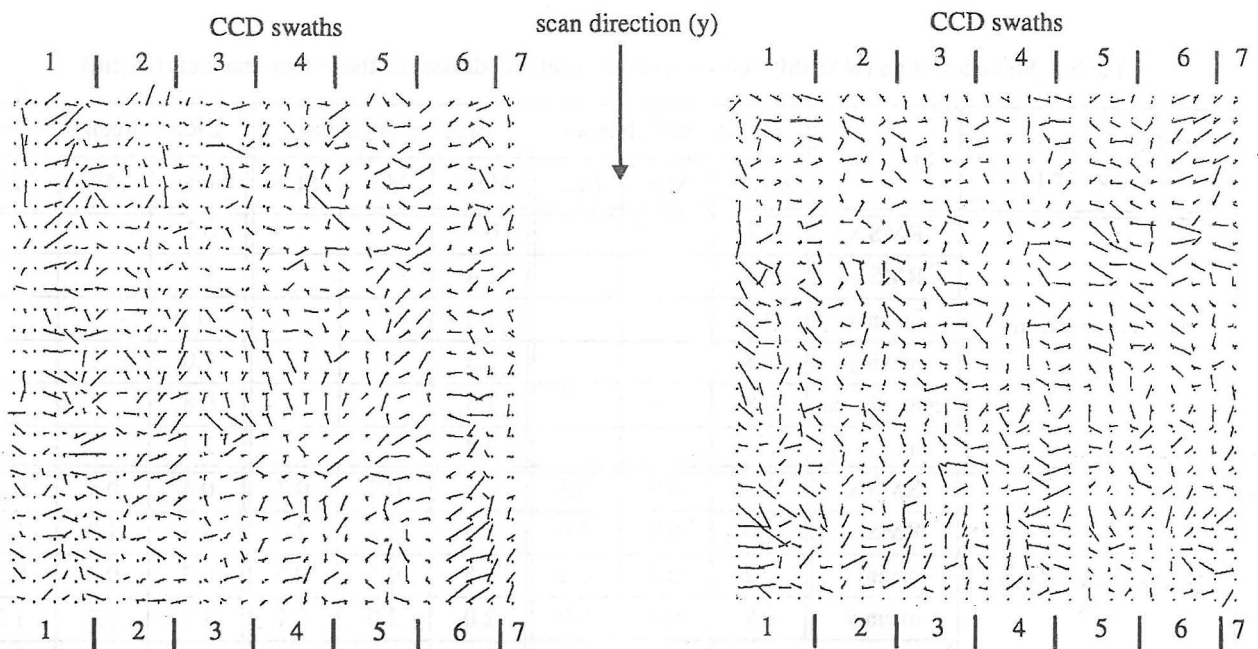


Figure 1. Residuals of affine transformation from pixel to reference coordinates using all 625 crosses as control points (red channel). Left SCAI1, right first scan of SCAI2. In both cases local systematic errors are clearly visible.

Table 1. Statistics of differences between pixel and reference coordinates after an affine transformation (in μm)

Scan version, # of control/check points	Statistics ¹	Red channel			Green channel			Blue channel		
		Mean	Min	Max	Mean	Min	Max	Mean	Min	Max
SCAI1, one scan, 625/0	RMS x	2.2			2.2			2.3		
	RMS y	2.0			2.1			2.1		
	max abs. x	6.1			6.0			6.2		
	max abs. y	7.5			7.6			7.1		
SCAI1, one scan, 4/621	RMS x	2.2			2.2			2.3		
	RMS y	2.9			2.9			3.3		
	mean x	-0.1			-0.1			-0.2		
	mean y	2.0			1.9			2.4		
	max abs. x	6.0			5.9			5.9		
	max abs. y	6.9			7.3			8.0		
SCAI2, three scans, 625/0	RMS x	2.3	2.1	2.4	2.3	2.1	2.5	2.3	2.2	2.5
	RMS y	2.0	2.0	2.1	2.1	2.0	2.1	2.1	2.0	2.1
	max abs. x	8.1	7.7	8.7	8.1	7.8	8.7	8.0	7.6	8.6
	max abs. y	6.3	6.1	6.7	6.6	6.3	6.8	7.0	6.5	7.4
SCAI2, three scans, 4/621	RMS x	2.8	2.4	3.2	2.8	2.5	3.2	2.8	2.5	3.2
	RMS y	2.3	2.2	2.3	2.3	2.2	2.3	2.3	2.2	2.4
	mean x	-1.2	-1.6	-0.8	-1.2	-1.6	-0.9	-1.2	-1.6	-0.9
	mean y	0.2	-0.4	1.0	0.3	-0.5	1.0	0.3	-0.3	1.2
	max abs. x	7.5	6.7	8.7	7.7	6.9	8.8	7.8	7.1	8.8
	max abs. y	6.5	6.0	6.7	6.5	6.2	6.8	6.4	6.2	6.5

¹ When all points are used as control points, the mean values are zero and thus not listed.

Table 2. Statistics of pairwise differences between pixel coordinates of the colour channels (in μm)

Scan version, # of comparison points	Statistics	Green - Red channel			Blue - Red channel			Blue - Green channel		
		Mean	Min	Max	Mean	Min	Max	Mean	Min	Max
SCAI1, one scan, 625	RMS x	0.2			0.4			0.2		
	RMS y	1.4			2.4			1.1		
	mean x	0.0			-0.1			-0.1		
	mean y	1.3			2.3			1.0		
	max abs. x	0.8			1.5			0.8		
	max abs. y	2.7			4.3			2.2		
SCAI2, three scans, 625	RMS x	0.3	0.3	0.3	0.7	0.7	0.7	0.4	0.4	0.4
	RMS y	1.0	0.9	1.0	2.3	2.2	2.3	1.3	1.3	1.3
	mean x	0.2	0.2	0.2	0.5	0.5	0.5	0.3	0.3	0.3
	mean y	0.9	0.8	0.9	2.0	2.0	2.1	1.2	1.2	1.2
	max abs. x	0.8	0.7	1.0	1.5	1.3	1.7	0.9	0.8	0.9
	max abs. y	2.1	2.0	2.1	4.3	4.1	4.5	2.7	2.6	2.9

3.2. Misregistration between Colour Channels

The results are summarised in Table 2 and one example is given in Figure 2. The errors are much larger in y than in x. The differences between the 3 scans (SCAI2) are very small. Generally the differences between the channels R, G, B are similar for G-R and B-G but quite larger for B-R (ca. the sum of G-R and B-G differences). The y-differences had always the same sign. This and also the large values of mean y (very similar to RMS y) show systematic errors in the scan direction. These errors are due to inaccurate mounting of the 3 CCD-lines on the CCD chip, i.e. the distance between the CCD lines is not exactly 294 μm . The error is larger between R and B and it becomes clearly visible when scanning with small pixel size sharp edges. As a test, a razor blade parallel to the CCD lines was scanned with 7 μm . The upper edge was blueish and the lower one reddish over the whole edge width of 5 pixels, and the differences between R and B were up to 40 grey values.

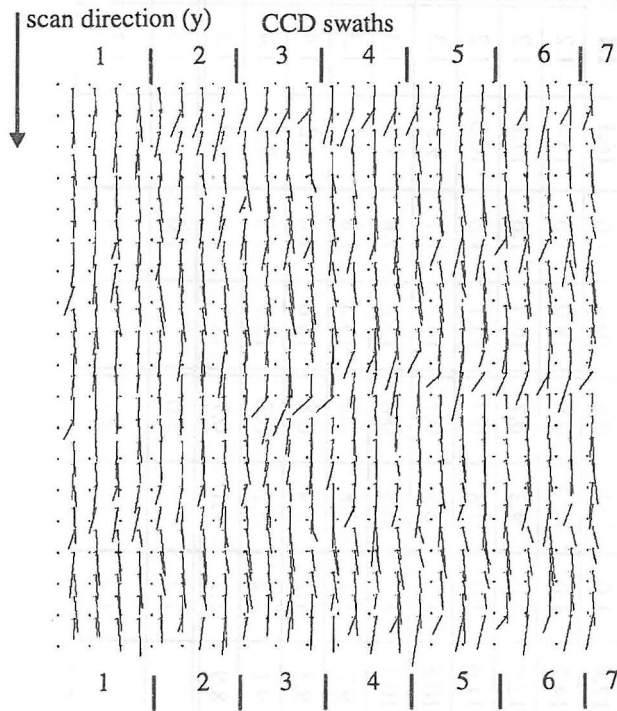


Figure 2. Colour misregistration errors, i.e. pixel coordinates of green minus red channel (SCAI1). The errors show a systematic constant y-shift between the two CCD-lines, while the x-errors are much smaller. This y-shift is due to inaccurate mounting of the CCD-lines, i.e. their distance is not 294 μm as specified.

3.3. Geometric Resolution

The smallest line group that could be sufficiently detected for both scanners had a line width of 7 μm (see Figure 3). Contrary to what was expected, the contrast of vertical lines (vertical was the scan direction) was clearly worse than that of the horizontal ones. Since the CCD sensor movement results in a smear and contrast loss, it was expected that the horizontal lines (i.e. parallel to the CCD) would have less contrast. A possible explanation is that the sensor integration time is less than the scan time required to sample a 7 μm pixel in scan direction, i.e. the effective y pixel

size is less than the nominal one.

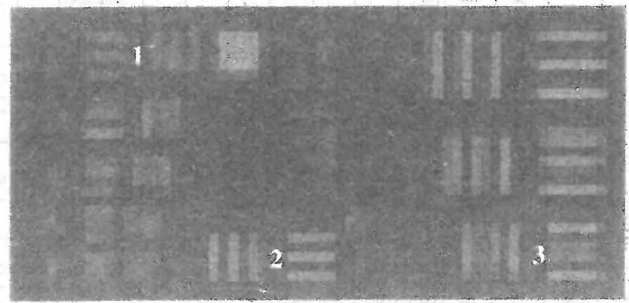


Figure 3. Visual determination of geometric resolution using the USAF resolution pattern scanned with 7 μm (SCAI2). The numbers 1, 2, 3 show lines with width 7, 8, and 9 μm respectively.

4. EVALUATION OF RADIOMETRIC PERFORMANCE

4.1. Noise, Linearity, Dynamic Range and Spectral Variation of Noise

The results from the grey scale wedge are shown in Table 3. With SCAI1 two problems occurred. Firstly, a very large number of pixels were rejected by the blunder test which excludes dust and corn, due to the very corny appearance of the scanned images. The number of rejected pixels was higher for the lower densities and reached up to ca. 50% (in comparison with SCAI2 0.6% of the pixels were rejected the most). Secondly, the scan parameters were not set appropriately and thus, the first two densities were saturated. Hence, the analysis will concentrate on the results of SCAI2. With SCAI2 the 14 μm version with exposure time 6 was of little use. The scanner does not adjust the scan parameters automatically when the exposure time is changed, and thus, due to the lower exposure time, the density range 0.05-3.09D was mapped to grey values 3-122, making a direct comparison to the version with exposure time 17 difficult. However, if the grey value range of the latter version is compressed to 3-122, then its noise is 32%-41% less than the noise of the version with exposure time 6, which makes clear the benefit of lower noise with longer exposure time. An example of the histogram of the grey scale for the red channel and 14 μm is shown in Figure 4.

The green channel has slightly more noise than the red one, and the blue one significantly more. The noise level is 1-1.6 and 0.9-1.3 for the 7 and 14 μm scans respectively. The 14 μm scans have slightly less noise than the 7 μm ones (11%-23% less noise), but still more than theoretically expected, i.e. twice ($=\sqrt{4}$) less. The noise is decreasing from low to high densities, but beyond the maximum detectable density even a slight increase can be observed. For high densities beyond 2D the standard deviation is higher than expected and observed with other scanners, but this also shows that even for the highest densities the signal is not saturated. The dynamic range, according to the criteria listed in section 2, is 1.6-1.9D and 1.75-2.05D for the 7 and 14 μm scans respectively, whereby R has a higher dynamic range than G and this than B. The plots in Figure 5 are in accordance with the above stated maximum detectable density and show a good linear behaviour up to this density. There are some differences between the 3 spectral scans, especially between B and the other two

Table 3: Radiometric tests with grey scale wedge. Mean and standard deviation of grey values. Maximum density that can be detected shown in bold.

Density	Red channel, SCAI2				Green channel, SCAI2				Blue channel, SCAI2				Red channel, SCAI1					
	7 μ m		14 μ m		7 μ m		14 μ m		7 μ m		14 μ m		7 μ m		14 μ m, version 1		14 μ m, version 2	
	Mean	St.D.	Mean	St.D.	Mean	St.D.	Mean	St.D.	Mean	St.D.	Mean	St.D.	Mean	St.D.	Mean	St.D.	Mean	St.D.
0.05	221.4	1.1	224.0	0.3	220.0	1.1	222.6	1.1	214.6	1.2	217.6	1.2	255.0	0.0	255.0	0.0	255.0	0.0
0.2	175.4	1.6	179.7	1.5	175.1	1.5	176.6	1.5	171.7	1.6	173.2	1.6	254.7	1.4	255.0	0.0	254.4	1.1
0.35	137.9	1.5	141.2	1.5	139.0	1.5	139.4	1.4	137.0	1.5	137.3	1.5	182.9	5.8	252.9	3.8	182.9	5.3
0.51	106.6	1.4	109.1	1.5	108.6	1.4	108.2	1.5	107.9	1.5	107.1	1.5	119.6	5.7	168.8	5.7	119.7	4.9
0.66	83.3	1.4	85.3	1.3	86.1	1.3	85.0	1.3	86.3	1.4	84.7	1.4	80.7	5.5	114.6	5.6	81.3	4.2
0.8	65.7	1.2	67.1	1.2	68.9	1.32	67.3	1.2	69.7	1.4	67.5	1.3	56.5	5.2	79.6	5.2	57.1	3.4
0.96	50.3	1.1	51.2	1.1	53.9	1.2	51.8	1.1	55.4	1.4	52.6	1.2	38.8	4.5	53.9	4.7	39.2	2.5
1.12	38.0	1.0	38.5	0.9	41.9	1.1	39.4	1.0	43.7	1.4	40.4	1.2	27.1	3.6	36.9	3.8	27.3	1.8
1.28	28.8	0.9	28.8	0.9	32.6	1.0	29.8	0.9	35.0	1.4	31.3	1.1	19.3	2.7	26.0	2.8	19.5	1.3
1.44	22.0	0.9	21.8	0.8	25.9	1.0	22.8	0.8	28.5	1.4	24.5	1.1	14.2	1.9	18.7	2.0	14.3	1.0
1.59	17.1	0.8	16.7	0.7	21.0	1.0	17.7	0.8	24.0	1.4	19.7	1.1	11.1	1.5	14.0	1.5	11.2	0.8
1.75	13.4	0.8	12.9	0.7	17.4	1.0	13.9	0.8	20.4	1.6	16.1	1.1	8.8	1.2	10.8	1.1	9.0	0.6
1.9	11.0	0.8	10.2	0.7	14.7	1.0	11.2	0.8	18.0	1.6	13.4	1.2	7.4	1.0	8.7	0.9	7.5	0.6
2.05	8.9	0.8	8.2	0.6	12.9	1.0	9.2	0.7	16.4	1.6	11.8	1.2	6.4	0.9	7.3	0.7	6.6	0.5
2.22	7.5	0.8	6.8	0.6	11.6	1.0	7.8	0.7	15.1	1.6	10.3	1.2	5.8	0.8	6.3	0.7	5.9	0.4
2.37	6.7	0.9	5.9	0.6	10.8	1.1	6.9	0.7	14.3	1.7	9.5	1.3	5.3	0.8	5.8	0.5	5.5	0.5
2.52	6.1	0.9	5.2	0.7	10.1	1.2	6.3	0.8	13.8	1.8	9.0	1.3	5.0	0.7	5.2	0.6	4.9	0.4
2.67	5.7	0.9	4.7	0.7	9.7	1.2	5.8	0.8	13.3	1.8	8.5	1.3	4.8	0.6	4.9	0.4	4.8	0.4
2.82	5.4	0.9	4.4	0.6	9.3	1.2	5.4	0.8	13.0	1.8	8.2	1.4	4.8	0.6	4.8	0.4	4.8	0.4
2.95	5.2	0.9	4.2	0.6	9.1	1.2	5.2	0.8	12.9	1.8	8.1	1.4	4.7	0.6	4.8	0.4	4.8	0.4
3.09	5.1	0.9	4.1	0.6	8.9	1.2	5.1	0.7	12.7	1.8	7.9	1.3	4.7	0.6	4.8	0.4	4.8	0.4
Mean St. D.		1.0		0.9		1.2		1.0		1.6		1.3		2.2		2.0		1.5
Mean St. D. (0.51-1.44D)		1.1		1.1		1.2		1.1		1.4		1.3		4.2		4.3		2.7

channels. All mean grey values were nicely monotonically decreasing even for the highest densities. The mean values are similar for all spectral channels, indicating a good colour balance. The biggest differences are between R and B and reach 7 grey values the most. The mean values are also similar between the 7 and 14 μm scans. The grey value range slightly decreases from R to G to B channels.

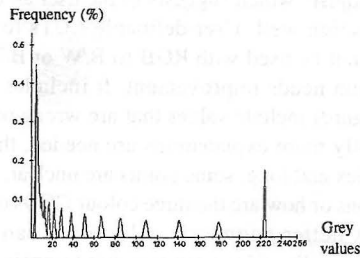


Figure 4. Histogram of grey scale for red scan, 14 μm , SCAI2. Frequencies are scaled by factor 3.9.

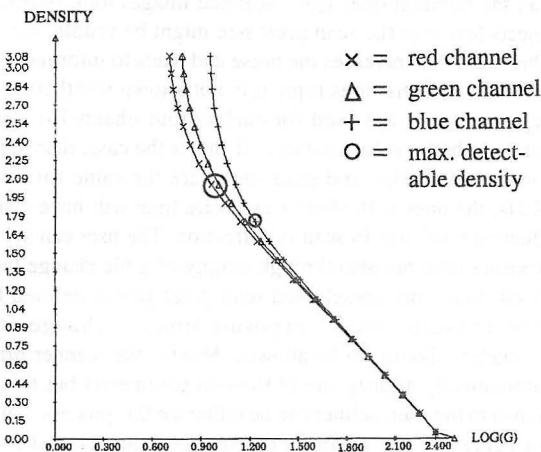


Figure 5. Grey scale linearity: 14 μm , exposure time 17, SCAI2.

A final note on some results of SCAI1 (see Table 3). There, it can be noticed that the 14 μm scan (version 1) had almost as much noise as the 7 μm scan which was contrary to what was expected. Also a visual comparison for low densities with a lot of corn did not show any difference. Thus, the 7 μm scan was subsampled by 2 x 2 averaging and “14 μm version 2” was created. This version does show, as expected, a significant decrease in noise. A possible explanation for the high noise of 14 μm version 1 may be that subsampling, at least in the scan direction, is not performed according to the manufacturer specifications, i.e. scanning speed or exposure time is less than it should be, thus resulting in practically smaller effective pixels.

4.2. Artifacts and Radiometric Problems

To detect artifacts visually the contrast of the scanned test patterns and the aerial films was strongly enhanced by Wallis filtering. For large images, first a subsampling by factor 2 has been performed. However, the quantification of radiometric errors always occurred in the original images. Figure 6 shows different artifacts. Figure 6 a) shows slightly bright, very bright and dark vertical stripes (observed with both scanners). In this

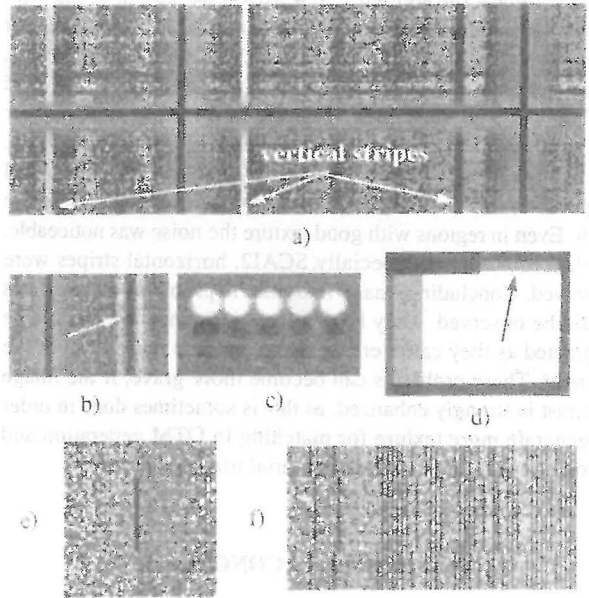


Figure 6. Artifacts and radiometric problems in contrast enhanced images (except d): a) vertical stripes (red channel, SCAI2); b) vertical black and white stripes (blue channel, SCAI1); c) inverse echoes due to multiplexing (blue channel, patterns at border of aerial film, SCAI1, scan direction is from top to bottom); d) grey region with height of 31 pixel in the scanned grey scale which did not physically exist. Presumably it is due to data losses during data transfer from scanner to host (red channel, 7 μm scan, SCAI1); e) sudden occurrence of a dark vertical line segment that does not physically exist with width of 2 pixels and height of 31 pixels. After this vertical line all pixels of these lines are shifted by two as the broken vertical stripes in f) clearly show. Again presumably due to data losses during data transfer (red channel, 7 μm scan, SCAI1); f) vertical dark stripes due to different response of the CCD sensor elements.

example the maximum mean difference between stripes and background was 1.9 grey values. These stripes occur at exactly the same x-positions for each scan swath, i.e. it seems that the CCD sensor element response differs due to inaccurate radiometric calibration. However, it is peculiar that the stripes have a width similar to the line width of the grid plate. Figure 6 b) shows bright/dark/bright vertical stripes. The mean difference between bright and dark stripes was 2.8 grey values and between bright stripes and background 2.5 grey values. We don't have an explanation for these errors. Figure 6 c) shows an inverse echo (signal duplication) in scan direction when scanning a colour aerial film. The distance between the echoes is 294 μm , i.e. equal to the distance between the CCD lines. Although the manufacturer claims that one read-out register and A/D converter is used for each CCD-line, it seems that this is not the case and due to multiplexing the signal from each CCD influences the remaining two. These echoes were observed with sharp edges and in this example the dark echoes led to a grey level difference to the background of up to 5 grey values. With SCAI2 no colour film was scanned but such effects were visible with the grid plate, however to a lesser extent, partly due to the thick grid lines that obscured the background (mean difference of echoes and background was 0.7 grey values). Figures 6 d), e) and f) show data losses during the transfer from scanner to host. The scanner

has its highest throughput (ca. 4 MB/s) for colour scans with 7 μm . Since the internal image buffer is small, if the data cannot be written to the host disk at this throughput rate data will be lost. Note that, in both cases, the data loss influenced 31 lines. Figure 6 f) shows also vertical stripes due to different CCD sensor element response. The mean difference of stripes to the background was up to 5 grey values. For both scanners the visual impression was that the noise in homogeneous regions was quite high. Even in regions with good texture the noise was noticeable. With both scanners, especially SCAI2, horizontal stripes were observed. Concluding, many radiometric problems and artifacts could be observed. They have a local influence but can not be neglected as they cause errors higher than the noise level of the scanner. These problems can become more grave, if the image contrast is strongly enhanced, as this is sometimes done in order to generate more texture for matching in DTM generation and automatic point measurement in aerial triangulation.

5. SUMMARY AND CONCLUSIONS

Regarding the geometric accuracy the RMS was 2-2.3 μm and the mean maximum absolute error 6-8.1 μm . The errors are bounded, i.e. the maximum absolute error is 2.7-3.6 RMS. Local systematic errors were observed with both scanners. The co-registration accuracy of colour channels is very good in x, but in scan direction there is a constant shift from one CCD to the next CCD line of ca. 1 μm due to fabrication inaccuracies. The shift between R and B channels is ca. 2.5 μm , i.e. more than the geometric accuracy of the scanner, and creates wrong colours at sharp edges with high resolution scans. The short term repeatability was very high. Both scanners had similar geometric accuracy values but one was better in x-direction, the other one in y. The use of a denser and more accurate grid plate will allow a better modelling and understanding of the magnitude and distribution of the errors. An effort to use a 1 cm thick plate with 2 mm grid spacing and 1 μm accuracy was not possible because SCAI can use plates only up to 4.5 mm thickness. The radiometric noise level is 1-1.6 and 0.9-1.3 grey values for 7 and 14 μm scan pixel size respectively. The dynamic range is 1.6-1.9D and 1.75-2.05D for 7 and 14 μm respectively with a good linear response up to this value. There were no significant differences between R, G, B channels with respect to geometry but their radiometric behaviour was quite different with B showing clearly a poorer quality, and G being slightly worse than R. Quite a lot of artifacts and electronic noise problems causing systematic local errors larger than the noise level of the scanner were observed. The most important are vertical stripes due to different CCD sensor element response because of inaccurate radiometric calibration, echoes due to multiplexed read-out of the signal from the 3 CCDs, and data losses due to high data generation rate. Latter problem also depends on the data transfer rate of the scanner/host interface as well as the host configuration and its simultaneous use by other programs. Tests at L+T with 7 μm scans of colour aerial images (host was a 180 MHz O2, R5000 processor, 128 MB RAM) did not show any such data losses, although the worst possible case has not been checked yet.

The software is generally positive and easy to handle. One major weakness is the lack of the ability to find automatically the darkest and lightest regions in an image and set appropriately the scan parameters. This feature is very important, especially for

good quality unattended roll film scanning, and is planned for a future software version. The unattended roll film scanning has been tested by scanning 400 images with different distances between the images particularly between flight strips. For all images the scanner software was able to detect automatically the area to be scanned. Automatic interior orientation works nicely, if the film orientation is given, but only for TLD format images. Images can be saved in TIFF format but only in the tiled option. An option "adjust" which suggests to the user an exposure time does not function well. User-definable LUTs for each colour channel can not be used with RGB to B/W or B/W scans. The documentation needs improvement. It includes half finished sentences, figures include values that are wrong or do not make sense, partially more explanations are needed, the part on roll film is complex and long, some points are unclear, e.g. regarding the calibrations or how are the three colour CCDs used with B/W scans etc. A better geometric calibration can improve the accuracy, especially if inaccuracies due to ageing effects start occurring. A compulsory radiometric normalisation before each scan can lead to less vertical stripes. It is not clear how subsampling is performed, but there are several indications that, at least in the scan direction, the effective pixel size is smaller than the nominal one. Thus, scanned images look sharper, and objects less than the scan pixel size might be visible, but on the other hand this increases the noise and leads to information loss. Related to the previous topic it is not known whether different exposure times are used for each colour channel in order to achieve a better colour balance. If this is the case, then since the nominal pixel size and scan speed are the same for all three CCDs, the ones with shorter exposure time will have a smaller effective pixel size in scan (y) direction. The user can select the exposure time but also through editing of a file change the scan speed. Since the preselected scan pixel size is defined by the product (scan speed x exposure time), a change of both parameters should not be allowed. Maybe, the scanner firmware automatically adjusts one of the two parameters but this is not known to the user, neither can he influence this process. Although not necessary for scanning per se, good quality and possibly automated software modules for correction of vignetting and hot spots is very important in production environments, especially when scanning negatives.

Summarising, SCAI is a good quality scanner. Improvements, especially in close cooperation with users and researchers, are necessary and can lead to an even better performance.

REFERENCES

- Baltsavias, E. P., 1991. Multiphoto Geometrically Constrained Matching. Ph. D. dissertation, *Institute of Geodesy and Photogrammetry, ETH Zurich, Mitteilungen No. 49*, 221 p.
- Gruen, A., 1985. Adaptive Least Squares Correlation: a Powerful Image Matching Technique. *South African Journal of Photogrammetry, Remote Sensing and Cartography*, Vol. 14, No. 3, pp. 175-187.
- Mehlo, H., 1995. Photogrammetric Scanners. *Proc. of 45th Photogrammetric Week*, Institute for Photogrammetry, University of Stuttgart, Wichmann Verlag, Karlsruhe, pp. 11-17.
- Roth, G., 1996. Quality Features of a State-of-the-Art High-Performance Photogrammetric Scanning System: PHODIS SC. *Int'l Archives of Photogrammetry and Remote Sensing*, Vol. 31, Part B1, pp. 163-166.